^{15}N NMR Study of the Ionization Properties of the Influenza Virus Fusion Peptide in Zwitterionic Phospholipid Dispersions

Zhe Zhou,* Jed C. Macosko,[†] Donald W. Hughes,[‡] Brian G. Sayer,[‡] John Hawes,[§] and Richard M. Epand*[‡]

*Department of Biochemistry and [‡]Department of Chemistry, McMaster University, Hamilton, Ontario L8N 3Z5, Canada; [†]Department of Chemistry, University of California, Berkeley, California 94720 USA; and [§]Biochemistry Biotechnology Facility, University of Indiana, Indianapolis, Indiana 46202 USA

ABSTRACT   Influenza virus hemagglutinin (HA)-mediated membrane fusion involves insertion into target membranes of a stretch of amino acids located at the N-terminus of the HA$_2$ subunit of HA at low pH. The pK$_a$ of the α-amino group of ^{1}Gly of the fusion peptide was measured using ^{15}N NMR. The pK$_a$ of this group was found to be 8.69 in the presence of DOPC (1,2-dioleoyl-sn-glycero-3-phosphocholine). The high value of this pK$_a$ is indicative of stabilization of the protonated form of the amine group through noncovalent interactions. The shift reagent Pr^{3+} had large effects on the ^{15}N resonance from the α-amino group of Gly^1 of the fusion peptide in DOPC vesicles, indicating that the terminal amino group was exposed to the bulk solvent, even at low pH. Furthermore, electron paramagnetic resonance studies on the fusion peptide region of spin-labeled derivatives of a larger HA construct are consistent with the N-terminus of this peptide being at the depth of the phosphate headgroups. We conclude that at both neutral and acidic pH, the N-terminal of the fusion peptide is close to the aqueous phase and is protonated. Thus neither a change in the state of ionization nor a significant increase in membrane insertion of this group is associated with increased fusogenicity at low pH.

INTRODUCTION

Membrane fusion is involved in a wide variety of biological processes, from sperm-oocyte fusion, to myoblast fusion during muscle development, to intracellular membrane trafficking events, as well as infection by enveloped viruses.

Elucidation of the mechanism of membrane fusion is very important for understanding cellular processes. Influenza virus enters target cells by receptor-mediated endocytosis and is delivered to an intracellular acidic organelle, the endosome. The low pH of this compartment triggers a conformational change in the viral hemagglutinin protein (HA), rendering it fusion-active and thus promoting the merger between the viral envelope and the endosomal membrane (Melikyan and Chernomordik, 1997; Gaudin et al., 1995; White, 1995). Influenza virus HA, a homotrimeric glycoprotein synthesized in infected cells as an inactive precursor, designated HA$_0$, becomes fusion-competent after cleavage into two subunits, HA$_1$ and HA$_2$, which are joined by disulfide bonds (Wiley and Skehel, 1987). At neutral pH, HA trimers form spikes that project 130 Å from the viral envelope (Ramalho-Santos and Lima, 1998), each monomer containing a globular head region (HA$_1$), responsible for viral binding to sialic acid-containing receptors in target membranes, and an envelope-anchored stem region (HA$_2$). HA-mediated membrane fusion only takes place after a protein conformational change at low pH. This conforma-

tional change results in the exposure of a stretch of ~20 amino acids that are located at the N-terminus of HA$_2$. This is a consequence of the dissociation of the globular heads of the HA$_1$ subunit so as to allow formation of an extended coiled coil structure in the HA$_2$ subunit (White and Wilson, 1987; Carr and Kim, 1993). In addition, acidification results in the protonation of specific amino acid residues, including several in a newly formed kinked loop (Epand et al., 1999).

Although much information has been obtained on the structural properties of truncated forms of HA at neutral (Wilson et al., 1981) and acidic (Bullough et al., 1994) pH, the molecular mechanism of membrane fusion as mediated by the influenza HA is still not well understood (Ramalho-Santos and Lima, 1998). The role of the fusion peptide, located at the N-terminal of HA$_2$, in HA-mediated membrane fusion has long been thought to be required for the destabilization of the target membrane bilayer (Epand and Epand, 1994). Indeed, several studies have shown that it is the segment of the HA protein corresponding to the fusion peptide that can penetrate target membranes before fusion, suggesting that this might be the first step leading to lipid mixing (Tsurudome et al., 1992; Harter et al., 1989; Stegmann et al., 1991; Durrer et al., 1996).

Further evidence for the importance of the terminal amino group in viral fusion is that many viral fusion peptides occur at the amino terminus of a viral fusion protein. In addition, peptides blocked at the amino terminus are often found to inhibit viral fusion, while freeing the amino group can convert the peptide into one that promotes negative curvature strain (Epand et al., 1993), a property often associated with more rapid rates of membrane fusion. In addition, mutation of position 1 of HA produces a virus that is not infectious (Gething et al., 1986) and whose fusion peptide produces less negative curvature strain (Epand and Epand, 1994).

Two previous electron paramagnetic resonance (EPR) studies, one using a labeled N-terminal 20-amino acid fusion peptide and another using labeled cysteine mutants of a longer 127-amino acid trimeric HA$_2$ construct (FHA2), left some uncertainty regarding the location of the amino terminus of the fusion peptide when inserted into membranes. Using the FHA2 construct, it was suggested that the amino terminus was close to the membrane interface (Macosko et al., 1997). However, the conclusion was based on a series of eight spin-labeled cysteine mutants at positions 5–14 in the sequence, and no data were obtained from residues 1–4, which were assumed to be part of a continuous α-helix. Interestingly, this conclusion was in conflict with the other EPR study using a 20-amino acid peptide that was spin-labeled at the amino terminus (Lüneberg et al., 1995). That work suggested that the amino terminus might be inserted into the hydrophobic regions of the membrane. However, the chemical modification of the amino terminus caused by introduction of the spin label results in a loss of the positive charge at the amino terminus. One might therefore anticipate that this uncharged amino terminus would insert more deeply into the membrane. The present study directly monitors the pK$_a$ and solvent accessibility of the amino terminus of the fusion peptide, using ^{15}N NMR.

EXPERIMENTAL PROCEDURES

Materials

The phospholipid used in this study, 1,2-dioleoyl-*sn*-glycero-3-phosphocholine (DOPC), was purchased from Avanti Polar Lipids (Alabaster, AL). Deuterium oxide (99.9%), ^{15}N-labeled glycine (99%), and ^{15}NH$_4$NO$_3$ (98%) were purchased from Isotec (Miamisburg, OH). Praseodymium (III) chloride (99.99%) was obtained from Aldrich (Milwaukee, WI). Gadolinium chloride (99.9%) was bought from ICN Pharmaceuticals (Plainview, NY). The ^{15}N-labeled peptide was made by standard solid-phase synthetic methods, using fluoren-9-ylmethoxy carbonyl chemistry. The final purification of the peptide was on a Hamilton PRP-1 high-performance liquid chromatography column. The peptide was applied to the column in a solution of dimethyl sulfoxide, trifluoroethanol, and 0.1 M ammonium acetate (1:2:2, v:v:v), and the eluent was a gradient containing water, ammonium acetate, and acetonitrile, with increasing acetonitrile concentrations. The fractions containing the purified peptide were then lyophilized to dryness. The identity of the peptide was verified by fast-bombardment mass spectrometry and by amino acid analysis. The peptide synthesized is the fusion peptide of the X31 strain of influenza virus. The sequence is GLFGAIAGFIENGWEGMIDG-amide, with G^1 labeled with ^{15}N.

The three FHA2 cysteine mutants, corresponding to the ectodomain of the HA$_2$ subunit of HA, were all expressed, purified, and spin labeled following the procedure described previously (Macosko et al., 1997). Spin label concentrations were determined by comparing double integrals of the first derivative EPR spectra with that of a standard sample made of 100 μM 4-hydroxy Tempo. For all mutants the spin labeling ratios were nearly quantitative. Triton X-100 was purchased from Fischer Scientific (Fair Lawn, NJ). Nickel ethylenediaminediacetic acid (NiEDDA) was generously provided by Dr. Charles Russell. Spin-labeled phospholipids were purchased from Avanti Polar Lipids.

Sample preparation for NMR studies

CHCl$_3$/MeOH (2:1 v/v) was added to 10 mg ^{15}N-labeled peptide and 151.5 mg DOPC (peptide:lipid = 1:40 mol/mol), and the mixture was sonicated for 5 min in a bath-type sonicator. A homogeneous solution was achieved. The organic solvents were first removed with N$_2$ and then placed under vacuum overnight. To measure the pK$_a$ of the peptide in DOPC vesicles, 2 ml of 50 mM sodium phosphate buffer containing 100 mM NaCl in H$_2$O (pH 4.0) was used to hydrate the sample. The pH values were adjusted by titration with HCl and NaOH solutions. To use lanthanum ions, 2 ml of 10 mM sodium formate buffer was used to hydrate the sample, then the pH was adjusted to 5.00. The ^{15}N-labeled peptide concentration was 2.4 mM. The sample was sonicated with a bath-type sonicator for 60 min at 30°C. Because the peptide may exist both within as well as outside the small unilamellar vesicles (SUVs), the sample was sonicated for another 40 min after the pH was changed or lanthanum ions were added, before the NMR experiments.

Sample preparation for EPR studies

Lipid vesicles of uniform size (100 nm in diameter) containing DOPC, were made as previously described (Rabenstein and Shin, 1995). For the reconstitution, the vesicle solution was perturbed with 0.5% octyl glucoside (final concentration) and mixed with Triton X-100-solubilized spin-labeled FHA2 mutant protein. The final concentration of lipid in the mixture was 10 mM, and the protein concentration was 20 μM. The detergent was removed with Bio-Bead SM2 resin (BioRad, Hercules, CA), following a column protocol (Holloway, 1973). The reconstituted vesicles were obtained as a pellet by ultracentrifugation (100,000 $\times$ g for 1 h). The pellet was resuspended in buffer containing 100 mM NaCl and 50 mM sodium phosphate at pH 7.0.

NMR

^{15}N and ^{1}H NMR spectra were collected with coaxial NMR tubes on a Bruker DRX-500 at 30°C with a 10-mm liquid-state probe. ^{15}N-labeled ammonium nitrate dissolved in D$_2$O in the inner NMR tube of the coaxial NMR tubes was used as an external ^{15}N chemical shift reference at 0.0 ppm, with the D$_2$O serving as the lock signal.

EPR experiments

All EPR spectra were taken with the spin-labeled mutants reconstituted into large unilamellar phospholipid vesicles (1000 Å in diameter). EPR power saturation curves were generated as previously described (Macosko et al., 1997). The power saturation approach has been very useful for determining the topology and the secondary structure of membrane-binding peptides and proteins (Macosko et al.,

1997; Yu et al., 1994; Hubbell and Altenbach, 1994). For example, in a membrane/water system, the nonpolar region of a protein or peptide preferentially partitions into the membrane phase, while the polar region prefers the aqueous phase. Thus, depending on the location of the nitroxide spin label, its collision rate with a polar versus a nonpolar relaxing reagent will be different, which will give different power saturation curves.

Using spin-labeled mutants of bacteriorhodopsin, Hubbell and co-workers have recently developed a method to determine the immersion depth of the nitroxide from the membrane surface. The method is based on determining the ratio of the interaction of membrane-soluble (O_2) and of aqueous (M) relaxing reagents with the spin label, as determined by the power saturation curves in the presence of each reagent (Altenbach et al., 1994). It has been found that the natural log of this ratio is linearly proportional to the immersion depth.

In the present work, NiEDDA complex (final concentration 200 mM) was used as M, because it is a neutral, small ($M_r = 232$), water-soluble complex that is stable at low pH (only 1% free Ni^{2+} at pH 4). To remove all of the other nonspecific effects, we measure power saturation curves under N_2 flow conditions to obtain the interaction of nitroxides in the absence of any relaxing reagents.

RESULTS

Measurements of pK_a values of specific charge groups in peptides or proteins can be made directly with NMR by monitoring the chemical shift of a pertinent nucleus as a function of pH (Zhu et al., 1995). In particular, in the case of the influenza virus fusion peptide, the pK_a value of the Gly[1] residue can be obtained from such measurements by using a peptide isotopically enriched with ^{15}N on the α-NH_2 group. Because the number of hydrogen atoms bonded to the nitrogen nucleus of this residue changes with pH, its chemical shift is highly sensitive to the state of ionization of the residue.

We confirmed that we could accurately determine the pK_a of Gly, using ^{15}N NMR with coaxial NMR tubes. The ^{15}N NMR of a model sample of 48 mM ^{15}N-labeled glycine in buffer in the outer NMR tube (50 mM sodium phosphate and 100 mM NaCl) was measured as a function of pH (Fig. 1). To improve the signal-to-noise ratio, proton decoupling was used from pH 4.45 to pH 7.35. In this pH range, the labile proton exchange should not be very fast, and an NOE (nuclear Overhauser effect) was expected. It is obvious that the signal of the ^{15}N-labeled glycine in buffer has a phase different from that of the signal of [15]NH_4NO_3 in D_2O. This phenomenon is uncommon, but it is not difficult to understand because ^{15}N has a negative gyromagnetic ratio. Most protons of [15]NH_4NO_3 in D_2O were replaced by deuterium, and there is little NOE when proton decoupling is used. The NOE for the [15]NH_4NO_3 in D_2O in the inner NMR tube must
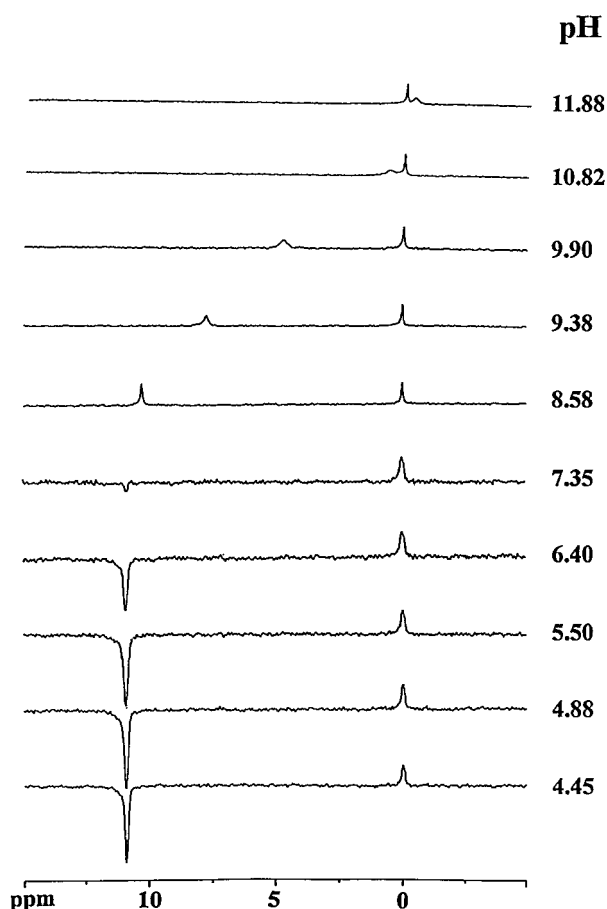

FIGURE 1   ^{15}N NMR spectra of 48 mM [^{15}N]Gly in 50 mM sodium phosphate and 100 mM NaCl as a function of pH. [15]NH_4NO_3 in D_2O in the inner NMR tube of coaxial NMR tubes was used as a reference.

be between -1 and 0 because a positive peak is observed for this resonance. But the situation is different for ^{15}N-labeled glycine in buffer in ordinary H_2O (in outer NMR tube), where there is a strong negative NOE effect. The NOE should be $-4.93 = NOE < -1$ because a negative peak is observed.

To confirm the above explanations, further experiments were conducted. ^{15}N NMR of 48 mM ^{15}N-labeled glycine in buffer in the outer NMR tube (50 mM sodium phosphate and 100 mM NaCl, pH 4.0) and [15]NH_4NO_3 in D_2O in the inner NMR tube were measured without (Fig. 2 a) and with (Fig. 2 b) proton decoupling. It is obvious that the two peaks have the same phase in Fig. 2 a but have different phases in Fig. 2 b. ^{15}N NMR of 48 mM ^{15}N-labeled glycine in 48 mM citrate buffer in the outer NMR tube (pH 4.0) and [15]NH_4NO_3 in D_2O in the inner NMR tube were also measured in the presence of proton decoupling, both without (Fig. 2 c) and with (Fig. 2 d) 5.3 mM Gd^{3+}. The two peaks in Fig. 2 c have different phases but have the same phase in Fig. 2 d. It is known that in the presence of the relaxation reagent Gd^{3+}, proton-induced relaxation becomes relatively
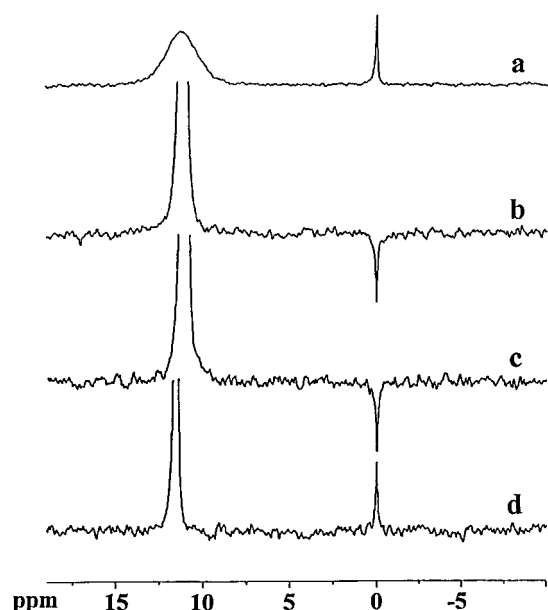
FIGURE 2 ^{15}N NMR of 48 mM [^{15}N]Gly in phosphate buffer (pH 4.0) without (*a*) and with (*b*) proton decoupling. (*c* and *d*) ^{15}N NMR of 48 mM [^{15}N]Gly in 48 mM citrate buffer (pH = 4.0) without (*c*) and with (*d*) 5.3 mM Gd^{3+}. ^{15}NH$_4$NO$_3$ in D$_2$O in the inner NMR tube of coaxial NMR tubes was used as a reference.

FIGURE 3 Nonlinear least-squares fit of the ^{15}N NMR chemical shifts (48 mM [^{15}N]Gly in 50 mM sodium phosphate and 100 mM NaCl) as a function of pH.

insignificant compared with electron-induced relaxation. As a consequence, the associated NOE is quenched (Sanders and Hunter, 1993). At higher pH, the NOE decreases because of the deprotonation (Fig. 1). The NOE is almost equal to −1 at pH 7.35. So the ^{15}N NMR spectra were measured without proton decoupling from pH 8.58 to pH 11.88.

The decrease of the chemical shift of ^{15}N-labeled glycine with increasing pH (Fig. 1) was fitted to the Henderson-Hasselbalch equation,

$$\delta = [\delta_{acid} + \delta_{base} \, 10^{pH-pK_a}]/[1 + 10^{pH-pK_a}]$$

where δ is the observed ^{15}N chemical shift at a specific pH and δ_{acid} and δ_{base} represent the chemical shift values at the low and high extremes of pH. A pK$_a$ of 9.81 was obtained by a nonlinear least-squares fit of the data (Fig. 3). The pK$_a$ value corresponds to the midpoint of the curve in Fig. 3. The pK$_a$ value obtained here with ^{15}N NMR is in excellent agreement with the published value of 9.78 (Weast, 1986).

Measurement of the ^{15}N NMR spectra of [^{15}N-^{1}Gly]-influenza virus fusion peptide in the presence of phospholipid is much more difficult than for the case of [^{15}N]glycine. Six to forthy-two hours was required to obtain one spectrum at a reasonable signal-to-noise ratio. The reasons for this are as follows: 1) The concentration of the peptide is 20-fold lower than that of [^{15}N]glycine. 2) The size of the peptide is large compared with [^{15}N]glycine. 3) The peptide binds to high-molecular-weight lipid vesicles. Fig. 4 *a* shows the ^{15}N NMR spectrum of the peptide/DOPC at pH
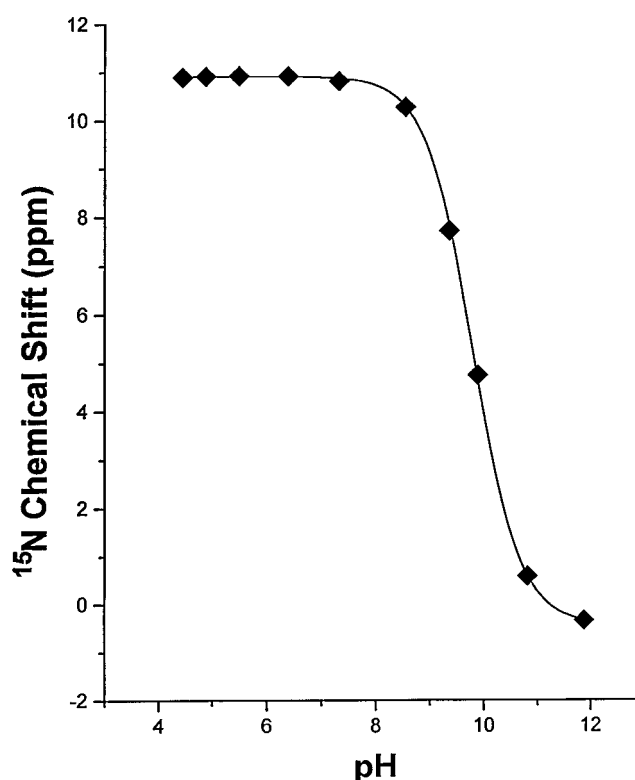
4.18. The ^{15}N signal of the peptide (in outer NMR tube) has a different phase compared with the signal of the reference, ^{15}NH$_4$NO$_3$ in D$_2$O in the inner NMR tube, because proton decoupling was used, as discussed above. It can be seen that the chemical shift is 7.5 ppm. Fig. 4 *b* is the ^{15}N NMR spectrum of the peptide/DOPC at pH 10.30. The ^{15}N signal of the peptide has the same phase compared with the signal of the reference because proton decoupling was not used (see above). The chemical shift at this pH is −4.8 ppm. Fig. 5 shows the dependence of the ^{15}N chemical shift of the peptide in the presence of DOPC on the pH. From a least-squares fit to this titration curve (Fig. 5), a pK$_a$ of 8.69 was obtained. The fit of the data to a theoretical titration curve was excellent and indicated that the error in the measured pK$_a$ was no greater than ±0.03. The pK$_a$ of [^{15}N]Gly-peptide in the presence of DOPC is significantly higher than that reported for other amino-terminal groups in peptides. For example, the pK$_a$ of the α-NH$_2$ group of penta-Gly is 8.02 (Weast, 1986), 0.67 pH units lower than that found for the fusion peptide. This shift is opposite the direction expected for insertion of the amino group of the fusion peptide into a more hydrophobic environment of the membrane. There are two factors that can explain the observed shift of pH value. One is the role of membrane surface charge in altering the interfacial pH, according to electrical double-
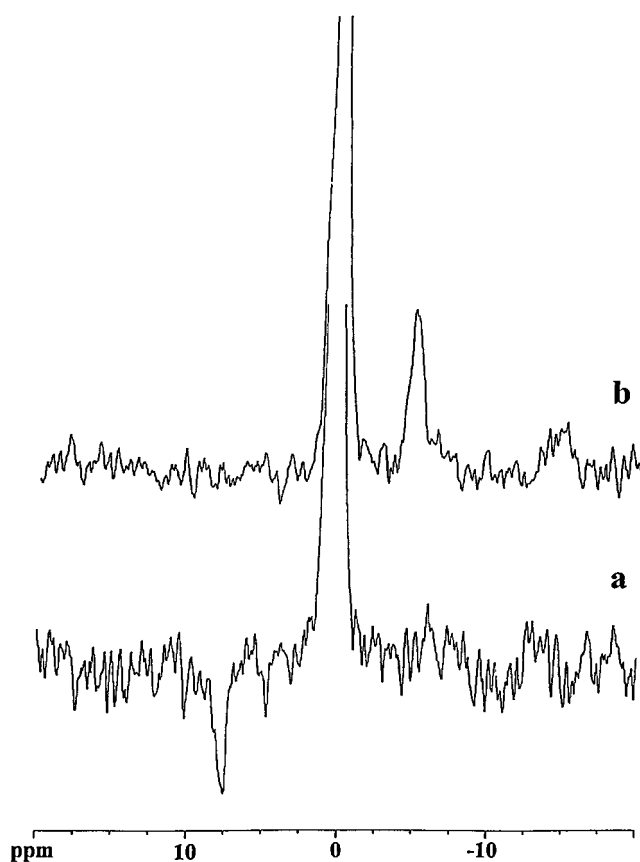
FIGURE 4 ^{15}N NMR spectra of [^{15}N]^{1}Gly influenza virus fusion peptide/DOPC (1:40, mol/mol) in 50 mM sodium phosphate and 100 mM NaCl. (*a*) pH 4.18; (*b*) pH 10.30. ^{15}NH$_4$NO$_3$ in D$_2$O in the inner NMR tube of coaxial NMR tubes was used as a reference.

FIGURE 5 Nonlinear least-squares fits of the ^{15}N NMR chemical shifts ([^{15}N]^{1}Gly influenza virus fusion peptide/DOPC in 50 mM sodium phosphate and 100 mM NaCl) as a function of pH.

layer effects described by the Gouy-Chapman theory (McLaughlin, 1989). The lipid is zwitterionic. However, the peptide has three negatively charged carboxyl groups in the pH range at which the amino group titrates. Because the binding of the peptide is relatively independent of pH (Rafalski et al., 1991), the membrane surface charge would be negative, at least above pH 7, making the surface pH lower than the bulk pH. However, with only 2.4 mM peptide (2 mol%) and a maximum of three negative charges per peptide, this effect will be small. For example, the pK$_a$ of the N-terminal Gly of melittin in micelles is 7.90 (Zhu et al., 1995), close to the value of 8.02 for penta-Gly, even though melittin is a peptide with six cationic groups. Changes in the interfacial pH may contribute to the observed shift in the pK$_a$ of the terminal amino group of the fusion peptide to higher values, but this is not the entire explanation. We therefore suggest that another factor contributing to the shift of pK$_a$ to higher values is the interaction of the α-NH$_3^+$ group with a negative charge, i.e., an electrostatic interaction stabilizing the protonated form. Thus, the α-NH$_3^+$ group of the peptide may bond with one of the carboxyl

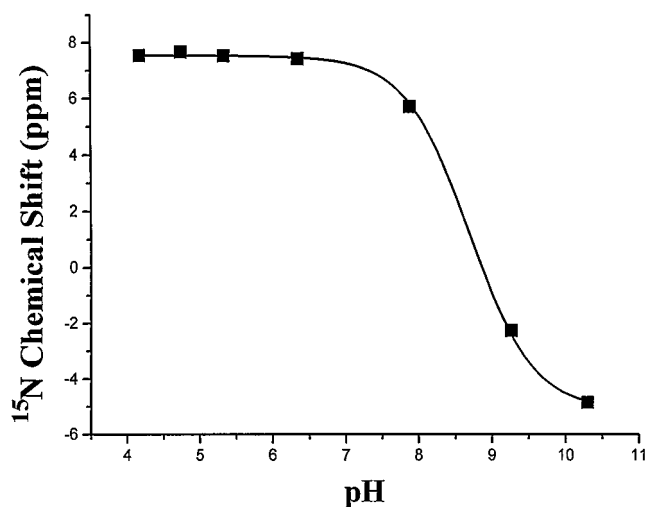groups of the peptide or with the phosphate group of the DOPC.

We further tested the degree of exposure of the terminal amino group of the membrane-inserted peptide to water-soluble cations. ^{1}H and ^{15}N NMR of [^{15}N]Gly-peptide/DOPC vesicles was measured in the presence of the shift reagent, Pr^{3+}, placed in the outer section of a coaxial NMR tube, and the pH was adjusted to 5.00. Fig. 6 *A* shows the ^{1}H NMR of the [^{15}N]Gly-peptide/DOPC (1:40 mol/mol) at pH 5.0 at different Pr^{3+} concentrations. Choline methyl and choline methylene signals were shifted as expected, because they are at the membrane surface. Signals from protons in the middle of the bilayer were not affected. Although the samples were sonicated for 40 min after additions of Pr^{3+}, at 5.0 and 10.0 mM Pr^{3+}, some of the SUVs appear to still only have very low concentrations of Pr^{3+} inside the vesicle (Fig. 6 *A*; the chemical shift of a fraction of the choline methyl groups was not affected).

Changes in the chemical shift in the presence of Pr^{3+} could be a consequence of a change in the bulk magnetic susceptibility (BMS). Because the CH$_3$ group of the acyl chain should be affected only by BMS when Pr^{3+} was added to the sample, the absolute chemical shift change of the CH$_3$ group of the acyl chain was used to calculate the BMS. The BMS is 0.08, 0.18, and 0.38 ppm when the Pr^{3+} concentration is 5, 10, and 20 mM, respectively. Fig. 6 *B* shows the ^{15}N NMR of [^{15}N]Gly-peptide/DOPC in the outer NMR tube (1:40 mol/mol) at pH 5.0 at different Pr^{3+} concentrations. The peak at 0.00 ppm is from ^{15}NH$_4$NO$_3$ in D$_2$O in the inner NMR tube. It is obvious that the ^{15}N signal of [^{15}N]Gly-peptide/DOPC was shifted to higher frequency. The chemical shift change is 0.27, 0.51, and 0.83 ppm at 5, 10, and 20 mM Pr^{3+}, respectively. The shift is much bigger than the BMS at corresponding Pr^{3+} concentrations.

A

Pr³⁺/mM

0.00

5.00

10.00

20.00

3.5 3.0 2.5 2.0 1.5 ppm

B

Pr³⁺/mM

0.00

5.00

10.00

20.00

10 8 6 4 2 0 -2 ppm

FIGURE 6 ¹H (A) and ¹⁵N (B) NMR of [¹⁵N]Gly-peptide/DOPC (1:40 mol/mol) at pH 5.0 at different Pr³⁺ concentrations.
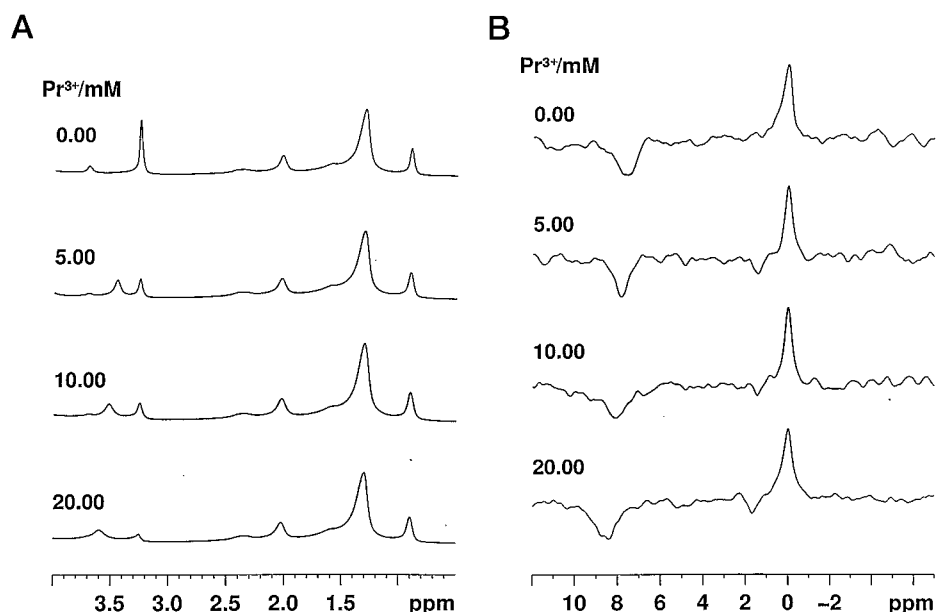
The membrane immersion depths based on EPR power saturation are described in the Experimental Procedures section. The resulting depths at pH 7.0 and 5.0 of the nitroxide spin labels attached to each mutant are plotted in Fig. 7. These depth measurements are consistent with previous measurements of the same mutants in SUVs (100 nm in diameter) containing 80 mol% palmitoyloleoylphosphati-
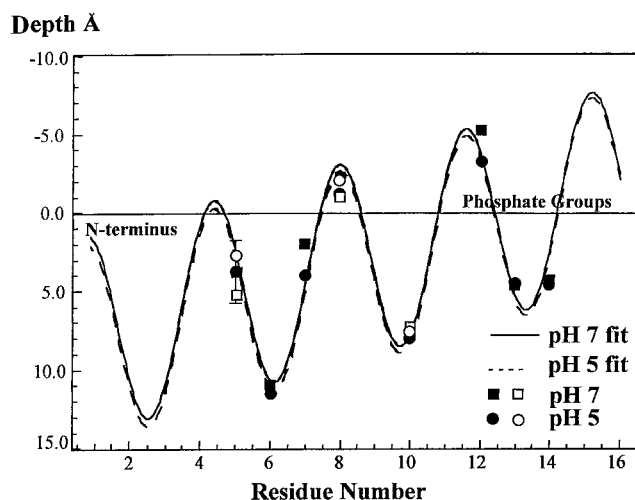
Depth Å

FIGURE 7 A plot of the measured depths at three residues of the DOPC-bound FHA2 fusion peptide region (○, □) and eight residues of the POPC/POPG (4:1)-bound FHA2 (●, ■). The fitted curves are based on a rigid α-helix (5.41-Å pitch and 1.50-Å translation per residue). The paramagnetic center is assumed to be extended 7 Å along a line connecting the central helical axis and the β-carbon of the cysteine. The calculated tilt angles based on all of the data are 25° and 28° from the plane of the membrane for pH 7 and pH 5, respectively. This orientation of the helix would position the N-terminal glycine at the phosphate headgroup region, consistent with the NMR data presented in this study.

dylcholine (POPC) and 20 mol% palmitoyloleoylphosphatidylglycerol (POPG) (Macosko et al., 1997). Together, these depth measurements reflect what would be expected from an α-helix buried in the membrane at an oblique angle.

Therefore, it was possible to fit these depth data into a standard α-helix model of a 5.41-Å pitch and 1.50-Å translation per residue (Fig. 7). We found that the best fitting tilt angles from the horizontal plane of the membrane are 25° for pH 7.0 and 28° for pH 5.0, respectively. The best fit for the helix rotation was consistent with its hydrophobic moment calculated based on recently determined hydrophobicities of amino acid residues (Thorgeirsson et al., 1996). In the model α-helix, the paramagnetic center in the nitroxide moiety is located 7 Å from the center axis of the helix backbone, and the nitroxide side chain is assumed to be extended along the line connecting the central helical axis and the β-carbon in cysteine.

We are interested in characterizing any topological change that may take place in the fusion peptide at low pH. In Fig. 7, the depth profiles of the fusion peptide region at pH 7 and pH 5 are quite similar. In fact the calculated angles differ by only 3°. This similarity is evidence that the fusion peptide region of the HA₂ domain does not undergo any conformational change or change in angle of insertion in the membrane as a function of pH.

DISCUSSION

There has been limited application of ¹⁵N NMR methods to obtain the dissociation constant of N-H protons. The pK$_a$ values of these groups are perturbed by electrostatic interactions with other charged groups as well as by the polarity of the environment of these groups. In the case of the

influenza fusion peptide, the terminal amino group has a pK$_a$ of 8.69 in the presence of liposomes. This value is high for a terminal amino group and suggests that the charged terminus of the peptide interacts with an anionic moiety. However, the protonation of this group plays no role in membrane fusion because its state of ionization does not change between the fusion-inactive pH of 7.4 and pH 5, where the rate of fusion is enhanced. It has been reported that the influenza HA protein can induce fusion even at neutral pH under denaturing conditions of high temperature or the presence of urea (Carr et al., 1997). The difference in the rate of fusion at neutral and acid pH is not affected by the state of ionization of the terminal amino group that remains the same.

We can also estimate whether the terminal amino group of the peptide remains accessible to the aqueous phase when it interacts with a membrane bilayer. The effect of lanthanide ions on the ^{15}N NMR spectra suggests that the terminal amino group remains close to the membrane surface, even at acidic pH. There is evidence, however, from the shift in the emission maximum of the Trp residue of this peptide, from 347 nm at pH 7.4 to 330 nm at pH 5.0, in the presence, but not in the absence, of liposomes of phosphatidylcholine (Rafalski et al., 1991; Lear and DeGrado, 1987) that there is a deeper insertion of the peptide at low pH. However, fluorescence quenching experiments of Trp argue against this conclusion and are in accord with the suggestion that there is no change in the depth of insertion of the peptide with pH (Clague et al., 1991). An alternative role of acidification is that the protonation of the acidic amino acid residues in the fusion peptide region allows for closer proximity in the membrane by lowering the electrostatic repulsion. A somewhat analogous situation occurs with succinylated melittin. This peptide cannot induce fusion at neutral pH but causes a rapid and efficient fusion at acidic pH concomitant with protonation of the carboxyl groups (Murata et al., 1987). The unmodified melittin, which does not contain the carboxyl groups of succinate, induces fusion in a pH-independent manner (Morgan et al., 1983; Eytan and Almary, 1983).

Using synthetic peptides corresponding to the N-terminus of several HAs, both α-helical and β-strands were detected, with a slight predominance of the former structure (Gray et al., 1996). It has been reported that these small, synthetic fusion peptides insert into target membranes at an oblique angle as an α-helix (Gray et al., 1996; Lüneberg et al., 1995). Moreover, the membrane topology of a homotrimeric, 14-kDa HA$_2$ construct, FHA2, was determined by EPR techniques (Macosko et al., 1997). The fusion peptide region of this construct, which promotes lipid mixing in conditions and at rates identical to those of native HA (Epand et al., 1999), was found to be locally monomeric and tilted 30° with respect to the plane of an anionic membrane. Because the influenza fusion peptide has charged groups that may interact with charges in the lipid headgroup, it was

important to test whether the conformation and the extent and angle of membrane insertion of the peptide were the same in zwitterionic as in anionic lipids. In the present study it is shown that the mode of insertion of the fusion peptide is not sensitive to the presence of anionic lipids. This mode of insertion also explains how the terminal amino group can be close to the membrane interface, even though the peptide is inserted into the membrane with the amino group entering first. It is a consequence of one face of the α-helix, which includes the N-terminal Gly residue, being oriented toward the aqueous phase (Fig. 7).

The results show that the α-NH$_2$ group remains protonated between a pH of 5 and 7.4. However, at pH 5 but not at pH 7, this peptide is active in promoting formation of a cubic phase in certain lipids (Colotto and Epand, 1997) and in promoting lipid mixing at very high peptide concentrations (Lear and DeGrado, 1987). The only groups on the peptide that are likely to change their state of ionization between neutral and acid pH are the three side-chain carboxyl groups. The protonation of these groups is suggested not to change the angle of insertion of the peptide into bilayers (Lüneberg et al., 1995), and it does not significantly affect the depth of burial of the fusion peptide in the membrane (Macosko et al., 1997, and the present work). It should be pointed out, however, that these acidic amino acids are not required for fusion and they can be replaced by mutagenesis (Steinhauer et al., 1995). The fact remains that under physiological conditions the rate of fusion promoted by the native HA molecule is greatly increased by acidification. From this paper and our earlier work (Macosko et al., 1997) it appears that the nature of the insertion of the fusion peptide into a membrane is not significantly affected by pH, and the terminal amino group remains protonated and exposed to the aqueous environment, even at acidic pH. Because much of the fusion peptide is positioned in the most rigid and tightly packed region of the bilayer, it is possible that small changes in the depth or angle of insertion of the peptide can have marked effects on the properties of the membrane. Alternatively, at neutral pH, the three ionized carboxyl groups on the exposed face of the fusion peptide region could prevent the fusion peptide-bound membrane from coming in close proximity to the target membrane because of electrostatic repulsion and/or an increased hydration barrier. ^{1}H NMR shows that vesicles do not aggregate at neutral or basic pH (data not shown). At acidic pH, membranes are aggregated by the peptide, aided by the loss of electrostatic repulsion. Furthermore, the change in peptide charge would favor more negative intrinsic curvature, thereby destabilizing the membrane and facilitating the formation of the initial fusion intermediate.

In summary, despite the importance of the amino terminus of HA$_2$ to membrane fusion, its state of ionization and position in the membrane are not significantly altered by a decrease in pH from 7 to 5.

REFERENCES

Altenbach, C., D. A. Greenhalgh, H. G. Khorana, and W. L. Hubbell. 1994. A collision gradient method to determine the immersion depth of nitroxides in lipid bilayers: application to spin-labeled mutants of bacteriorhodopsin. *Proc. Natl. Acad. Sci. USA.* 91:1667–1671.

Bullough, P. A., F. M. Hughson, J. J. Skehel, and D. C. Wiley. 1994. Structure of influenza haemagglutinin at the pH of membrane fusion. *Nature.* 371:37–43.

Carr, C. M., C. Chaudhry, and P. S. Kim. 1997. Influenza hemagglutinin is spring-loaded by a metastable native conformation. *Proc. Natl. Acad. Sci. USA.* 94:14306–14313.

Carr, C. M., and P. S. Kim. 1993. A spring-loaded mechanism for the conformational change of influenza hemagglutinin. *Cell.* 73:823–832.

Clague, M. J., J. R. Knutson, R. Blumenthal, and A. Herrmann. 1991. Interaction of influenza hemagglutinin amino-terminal peptide with phospholipid vesicles: a fluorescence study. *Biochemistry.* 30:5491–5497.

Colotto, A., and R. M. Epand. 1997. Structural study of the relationship between the rate of membrane fusion and the ability of the fusion peptide of influenza virus to perturb bilayers. *Biochemistry.* 36:7644–7651.

Durrer, P., C. Galli, S. Hoenke, C. Corti, R. Gluck, T. Vorherr, and J. Brunner. 1996. H$^+$-induced membrane insertion of influenza virus hemagglutinin involves the HA2 amino-terminal fusion peptide but not the coiled coil region. *J. Biol. Chem.* 271:13417–13421.

Epand, R. M., and R. F. Epand. 1994. Relationship between the infectivity of influenza virus and the ability of its fusion peptide to perturb bilayers. *Biochem. Biophys. Res. Commun.* 202:1420–1425.

Epand, R. M., R. F. Epand, C. D. Richardson, and P. L. Yeagle. 1993. Structural requirements for the inhibition of membrane fusion by carbobenzoxy-D-Phe-Phe-Gly. *Biochim. Biophys. Acta.* 1152:128–134.

Epand, R. F., J. C. Macosko, C. J. Russell, Y. K. Shin, and R. M. Epand. 1999. The ectodomain of HA2 of influenza virus promotes rapid pH dependent membrane fusion. *J. Mol. Biol.* 286:489–503.

Eytan, G. D., and T. Almary. 1983. Melittin-induced fusion of acidic liposomes. *FEBS Lett.* 156:29–32.

Gaudin, Y., R. W. H. Ruigrok, and J. Brunner. 1995. Low-pH induced conformational changes in viral fusion proteins: implications for the fusion mechanism. *J. Gen. Virol.* 76:1541–1556.

Gething, M. J., R. W. Doms, D. York, and J. White. 1986. Studies on the mechanism of membrane fusion: site-specific mutagenesis of the hemagglutinin of influenza virus. *J. Cell. Biol.* 102:11–23.

Gray, C., S. A. Tatulian, S. A. Wharton, and L. K. Tamm. 1996. Effect of the N-terminal glycine on the secondary structure, orientation, and interaction of the influenza hemagglutinin fusion peptide with lipid bilayers. *Biophys. J.* 70:2275–2286.

Harter, C., P. James, T. Bachi, G. Semenza, and J. Brunner. 1989. Hydrophobic binding of the ectodomain of influenza hemagglutinin to membranes occurs through the "fusion peptide." *J. Biol. Chem.* 264:6459–6464.

Holloway, P. W. 1973. A simple procedure for removal of Triton X-100 from protein samples. *Anal. Biochem.* 53:304–308.

Hubbell, W. L., and C. Altenbach. 1994. Site-directed spin labeling of membrane proteins. *In* Membrane Protein Structure: Experimental Approaches. Oxford University Press, New York. 224–248.

Lear, J. D., and W. F. DeGrado. 1987. Membrane binding and conformational properties of peptides representing the NH$_2$ terminus of influenza HA-2. *J. Biol. Chem.* 262:6500–6505.

Lüneberg, J., I. Martin, F. Nubler, J.-M. Ruysschaert, and A. Herrmann. 1995. Structure and topology of the influenza virus fusion peptide in lipid bilayers. *J. Biol. Chem.* 270:27606–27614.

Macosko, J. C., C.-H. Kim, and Y.-K. Shin. 1997. The membrane topology of the fusion peptide region of influenza hemagglutinin determined by spin-labeling EPR. *J. Mol. Biol.* 267:1139–1148.

McLaughlin, S. 1989. The electrostatic properties of membranes. *Annu. Rev. Biophys. Biophys. Chem.* 18:113–136.

Melikyan, G. B., and L. V. Chernomordik. 1997. Membrane rearrangements in fusion mediated by viral proteins. *Trends Microbiol.* 5:349–355.

Morgan, C. G., H. Williamson, S. Fuller, and B. Hudson. 1983. Melittin induces fusion of unilamellar phospholipid vesicles. *Biochim. Biophys. Acta.* 732:668–674.

Murata, M., K. Nagayama, and S. Ohnishi. 1987. Membrane fusion activity of succinylated melittin is triggered by protonation of its carboxyl groups. *Biochemistry.* 26:4056–4062.

Rabenstein, M. D., and Y. -K. Shin. 1995. A peptide from the heptad repeat of human immunodeficiency virus gp41 shows both membrane binding and coiled-coil formation. *Biochemistry.* 24:13390–13397.

Rafalski, M., A. Ortiz, A. Rockwell, L. C. Van Ginkel, J. D. Lear, W. F. DeGrado, and J. Wilschut. 1991. Membrane fusion activity of the influenza virus hemagglutinin: interaction of HA2 N-terminal peptides with phospholipid vesicles. *Biochemistry.* 30:10211–10220.

Ramalho-Santos, J., and M. C. P. Lima. 1998. The influenza virus hemagglutinin: a model protein in the study of membrane fusion. *Biochim. Biophys. Acta.* 1376:147–154.

Sanders, J. K. M., and B. K. Hunter. 1993. Connections through space. *In* Modern NMR Spectroscopy: A Guide for Chemists. Oxford University Press, Oxford. 178.

Stegmann, T., J. M. Delfino, F. M. Richards, and A. Helenius. 1991. The HA2 subunit of influenza hemagglutinin inserts into the target membrane prior to fusion. *J. Biol. Chem.* 266:18404–18410.

Steinhauer, D. A., S. A. Wharton, J. J. Skehel, and D. C. Wiley. 1995. Studies of the membrane fusion activities of fusion peptide mutants of influenza virus hemagglutinin. *J. Virol.* 69:6643–6651.

Thorgeirsson, T. E., C. J. Russell, D. S. King, and Y.-K. Shin. 1996. Direct determination of the membrane affinities of individual amino acids. *Biochemistry.* 35:1803–1809.

Tsurudome, M., R. Gluck, R. Graf, R. Falchetto, V. Schaller, and J. Brunner. 1992. Lipid interactions of the hemagglutinin HA2 NH$_2$-terminal segment during influenza virus-induced membrane fusion. *J. Biol. Chem.* 267:20225–20232.

Weast, R. C., editor. 1986. CRC Handbook of Chemistry and Physics. CRC Press, Boca Raton, FL. D159–D160.

White, J. M. 1995. Membrane fusion: the influenza paradigm. *Cold Spring Harb. Symp. Quant. Biol.* 50:365–394.

White, J. M., and I. A. Wilson. 1987. Anti-peptide antibodies detect steps in a protein conformational change: low-pH activation of the influenza virus hemagglutinin. *J. Cell. Biol.* 105:2887–2896.

Wiley, D. C., and J. J. Skehel. 1987. The structure and function of the hemagglutinin membrane glycoprotein of influenza virus. *Annu. Rev. Biochem.* 56:365–394.

Wilson, I. A., J. J. Skehel, and D. C. Wiley. 1981. Structure of the haemagglutinin membrane glycoprotein of influenza virus at 3 Å resolution. *Nature.* 289:366–373.

Yu, Y. G., T. E. Thorgeirsson, and Y. -K. Shin. 1994. Topology of an amphiphilic mitochondrial signal sequence in the membrane-inserted state: a spin labeling study. *Biochemistry.* 33:14221–14226.

Zhu, L., M. D. Kemple, P. Yuan, and F. G. Prendergast. 1995. N-terminus and lysine side chain pKa values of melittin in aqueous solutions and micellar dispersions measured by ^{15}N NMR. *Biochemistry.* 34:13196–13202.